Available online at www.sciencedirect.com
ScienceDirect
www.elsevier.com/locate/jmbbm

Research Paper

Influence of cross-link structure, density and mechanical properties in the mesoscale deformation mechanisms of collagen fibrils

Baptiste Depalle[a], *Zhao Qin*[a], *Sandra J. Shefelbine*[b], *Markus J. Buehler*[a,c,d,*]

[a]*Laboratory for Atomistic and Molecular Mechanics (LAMM), Department of Civil and Environmental Engineering, Massachusetts Institute of Technology, 77 Massachusetts Ave., Room 1-290, Cambridge, 02139 MA, USA*
[b]*Department of Mechanical and Industrial Engineering, Northeastern University, Boston, MA, USA*
[c]*Center for Computational Engineering, Massachusetts Institute of Technology, 77 Massachusetts, Ave. Cambridge, MA 02139, USA*
[d]*Center for Materials Science and Engineering, Massachusetts Institute of Technology, 77 Massachusetts Ave., Cambridge, MA 02139, USA*

ARTICLE INFO

Article history:
Received 3 June 2014
Accepted 7 July 2014
Available online 29 July 2014

Keywords:
Collagen
Fibril
Cross-links
Fracture
Nanomechanics
Molecular dynamics
Coarse-grained model

ABSTRACT

Collagen is a ubiquitous protein with remarkable mechanical properties. It is highly elastic, shows large fracture strength and enables substantial energy dissipation during deformation. Most of the connective tissue in humans consists of collagen fibrils composed of a staggered array of tropocollagen molecules, which are connected by intermolecular cross-links. In this study, we report a three-dimensional coarse-grained model of collagen and analyze the influence of enzymatic cross-links on the mechanics of collagen fibrils. Two representatives immature and mature cross-links are implemented in the mesoscale model using a bottom-up approach. By varying the number, type and mechanical properties of cross-links in the fibrils and performing tensile test on the models, we systematically investigate the deformation mechanisms of cross-linked collagen fibrils. We find that cross-linked fibrils exhibit a three phase behavior, which agrees closer with experimental results than what was obtained using previous models. The fibril mechanical response is characterized by: (i) an initial elastic deformation corresponding to the collagen molecule uncoiling, (ii) a linear regime dominated by molecule sliding and (iii) the second stiffer elastic regime related to the stretching of the backbone of the tropocollagen molecules until the fibril ruptures. Our results suggest that both cross-link density and type dictate the stiffness of large deformation regime by increasing the number of interconnected molecules while cross-links mechanical properties determine the failure strain and strength of the fibril. These findings reveal that cross-links play an essential role in creating an interconnected fibrillar material of tunable toughness and strength.

*Corresponding author at: Laboratory for Atomistic and Molecular Mechanics (LAMM), Department of Civil and Environmental Engineering, Massachusetts Institute of Technology, 77 Massachusetts Ave., Room 1-290, Cambridge, 02139 MA, USA.
E-mail address: mbuehler@mit.edu (M.J. Buehler).

http://dx.doi.org/10.1016/j.jmbbm.2014.07.008
1751-6161/

1. Introduction

Collagens constitute a family of proteins that represent the main component of connective tissue of vertebrates, making up about 25% to 35% of the body's protein content (Fratzl, 2008; Kadler et al., 2007). They are ubiquitous proteins responsible for maintaining the structural integrity and mechanical function of tissues in most multicellular organisms. Collagens have been identified in mammal tissues in more than 27 forms (Van der Rest and Garrone, 1991). The variety in their composition and organization satisfies the broad mechanical requirements for a range of function and loading conditions (Fratzl, 2008; Ottani et al., 2002). Among these different forms, type I collagen is the most abundant in the human body. It has a fibrillar structure that provides the structural basis to resist tensile, shear or compression forces and can mainly be found in structural tissues such as skin, tendons, ligaments, blood vessels cartilage and in the organic part of bones and teeth (Fratzl, 2008; Shoulders and Raines, 2009).

Most of the mechanical properties of these tissues depend on the nanostructure of collagen molecules and their interactions. The type I collagen molecule is composed of three polypeptides chains (two α_1 and one α_2 chains) that form a 300 nm long triple helix. The molecules assemble in a quarter-staggered fashion into thin (20–500 nm) and long (>1 mm) fibrils (Fratzl, 2008; Parry and Craig, 1977). In the fibrils, the tropocollagen molecules are entangled in a very particular fashion, as demonstrated recently by in situ by X-ray crystallography (Orgel et al., 2006; Nair et al., 2013; Gautieri et al., 2011). Collagen fibrils constitute the main building block of many structural tissues, such as bone ligament, tendon and skin.

The fibrillar structure is stabilized by several posttranslational modifications that allow the formation of intermolecular and interfibrillar cross-links. There are two main types of intermolecular cross-links. The first type is the result of an enzymatic reaction (Viguet-Carrin et al., 2006; Eyre and Wu, 2005; Bailey et al., 1998). It is initiated by the enzyme lysyl-oxidase acting on specific lysine amino-acids of the non-helical ends of a collagen molecule (N- or C-telopeptide; Knott and Bailey, 1998). The resulting allysine reacts with a specific lysine of an adjacent molecule to form an immature divalent intermolecular bond (Tanzer, 1968). Over time, these divalent cross-links further react with another telopeptide aldehyde group to form a trivalent mature bond linking three tropocollagen molecules (Viguet-Carrin et al., 2006; Eyre and Wu, 2005; Bailey et al., 1998). In addition to this main cross-link formation pathway, other cross-links may form from the reaction of allysines, lysines and histidines (Svensson et al., 2013).The second cross-link type results from Advanced Glycation End-products (AGEs). Unlike enzymatic cross-links that are confined in the terminal domains, AGEs can form in several locations along the length of the collagen (Gautieri et al., 2014). Most factors playing a role in the formation of AGEs remain unknown.

The multiple sources and pathways leading to AGEs formation and their wide variety of chemical structure are not fully characterized yet (Viguet-Carrin et al., 2006; Bailey et al., 1998; Bailey, 2001). It has been shown that enzymatic cross-links are essential in the formation and function of collagen fibrils by stabilizing the structure whereas AGEs accumulate with age and diabetes and may impair fibrils normal function (Bailey et al., 1998; Gautieri et al., 2014; Bailey, 2001). Indeed, the presence of AGEs leads to stiffening and a decrease of viscoelasticity of tendons (Galeski et al., 1977; Andreassen et al., 1981; Danielsen and Andreassen, 1988; Li et al., 2013), loss of plasticity and toughness in bone (Zimmermann et al., 2011; Tang and Vashishth, 2011), and stiffening and increased fragility in cartilage tissues (Verzijl et al., 2002).

In this study, we focus only on enzymatic cross-links. The concentration and chemistry of enzymatic cross-links in the matrix differs significantly depending on the tissue, location and age and are therefore thought to be function related (Eyre and Wu, 2005; Bailey et al., 1998). For example, in middle-age men, the density of trivalent cross-links range from 280 mmol/mol in skin (Saito et al., 1997), 495 mmol/mol in bone tissue (Saito et al., 1997; Wang et al., 2002; Viguet-Carrin et al., 2010), 870 mmol/mol in patellar tendon (Svensson et al., 2013, 2012; Couppé et al., 2009) up to 1800 mmol/mol in articular cartilage (Saito et al., 1997). Divalent cross-links density present a similar value across tissues around 1400 mmol/mol (Saito et al., 1997). This suggests that those characteristics of cross-links are critical for tuning material mechanical properties. It is for these reasons that we chose to study the role of the amount and type of enzymatic cross-links in defining the mechanical properties of collagen fibrils.

Experimental studies have investigated the relationship between cross-link density and type and the mechanical properties of collagen fibrils (Svensson et al., 2013; Li et al., 2013; Yang et al., 2012; Rigozzi et al., 2013; Fessel and Snedeker, 2009). The size and complex hierarchical structure of collagen fibrils pose challenges associated with quantifying the exact amount, type and distribution of cross-links present in the fibrils and to analyze extensively the deformation mechanisms involved. Simulation techniques represent an ideal tool to bring insight at the nanoscale where experimental techniques reach their limits. Full atomistic molecular modeling techniques have been used successfully to study the structure and mechanics of cross-linked tropocollagen molecules (Gautieri et al., 2014; Uzel and Buehler, 2011; Bourne and Torzilli, 2011). Full atomistic simulations are very powerful to aid in understanding the nanomechanical response of cross-linked molecules under loading but are far too expensive in computational resources to study fibril mechanics, where multiple molecules are included. Finite element simulations have been used to overcome these limitations (Siegmund et al., 2008), but the meshing constraints associated with the method make it almost impossible to retain important structural details associated with the hierarchical characteristics of the collagen fibril. Coarse-grained models represent a useful alternative to the expensive full-atomistic calculation and allow the reach of nanometer scale samples without considerably compromising the structure of the collagen molecules.

Two-dimensional coarse-grained models of idealized collagen fibrils have been previously developed to study the influence of molecule length, cross-link density and

mineralization on the mechanical behavior of the fibril (Buehler, 2007, 2008, 2006a). This simple model brought insight into the strength and failure mode of collagen fibril but cannot explain the three-phase behavior recently observed in experiments (Svensson et al., 2013). In order to refine the analysis of the mechanical behavior of the fibrils, we developed a three-dimensional coarse-grained model for the current study. Using full atomistic simulation results, we built a model of cross-linked collagen fibrils, respecting the geometry, entanglement and periodicity of each constituting tropocollagen molecule. The coarse grained model includes cross-links in their physiological location. The mechanical response of both collagen molecules and cross-links are accurately derived from reactive molecular dynamics simulations with atomistic resolution. Coarse graining allows significant scaling-up of the simulation capability, attaining length and time scales that are used in experiments. Using this three-dimensional model, we explored the influence of intermolecular cross-linking on the mechanical behavior of fibrils.

2. Material and methods

2.1. *Fibril model geometry*

The simulations performed in this study were generated using a mesoscopic model where solvated tropocollagen molecules are described as a collection of particles interacting according to multi-body potentials. Further details on the development of the mesoscopic model can be found in a series of previous publications (Buehler, 2006a, 2006b).

In the mesoscopic model, collagen microfibril geometry is based on Protein Data Bank entry 3HR2 representing the microfibrillar structure of type I collagen measured in situ by X-ray crystallography (Orgel et al., 2006). The full atomistic information of the triple helical tropocollagen molecule is simplified and represented as a single chain of 'beads' or 'super-atoms'. Every bead in the mesoscopic model represents several atoms of the full-atomistic model (Fig. 1). The influence of solvation water is also taken into account in the model. This simplification allows us to reach time scales of microseconds and length scales of several hundred nanometers that cannot be achieved using full-atomistic resolution. The coordinates of the atoms of a single tropocollagen molecule are averaged using spline approximation along the length of the molecule. Equidistant beads are then created along the spline to create the coarse-grained model (Fig. 1A and B). The distance between the beads is set to an equilibrium distance r_0 of 14.0 Å, which approximates the diameter of the tropocollagen molecule.

After aligning the molecule along its principal axis, the fibril is then built by replication of the tropocollagen to form a cylinder of diameter $d=20$ nm (Fig. 1D and E). The periodicity of the molecules is given by the X-ray crystallography measurement (Orgel et al., 2006). The model of the fibril is built to exhibit five gap/overlap regions along its length and is composed of 155 tropocollagen molecules which represent a total of 33,790 beads. The structure has been built to ensure its periodicity along the fibril axis (x-axis). During the simulation, the model is replicated by using periodic boundary conditions along its length to simulate an infinitely long fibril. The length of the model is larger than a single molecule length (~300 nm) in order to prevent artefactual interactions between the two ends of a molecule through the periodic boundaries. The collagen fibrils show the characteristic staggered arrangement as observed in experiments.

2.2. *Cross-links creation*

In this study, we focus on the role of enzymatic cross-links in the mechanics of collagen fibrils. Experimental analyses of

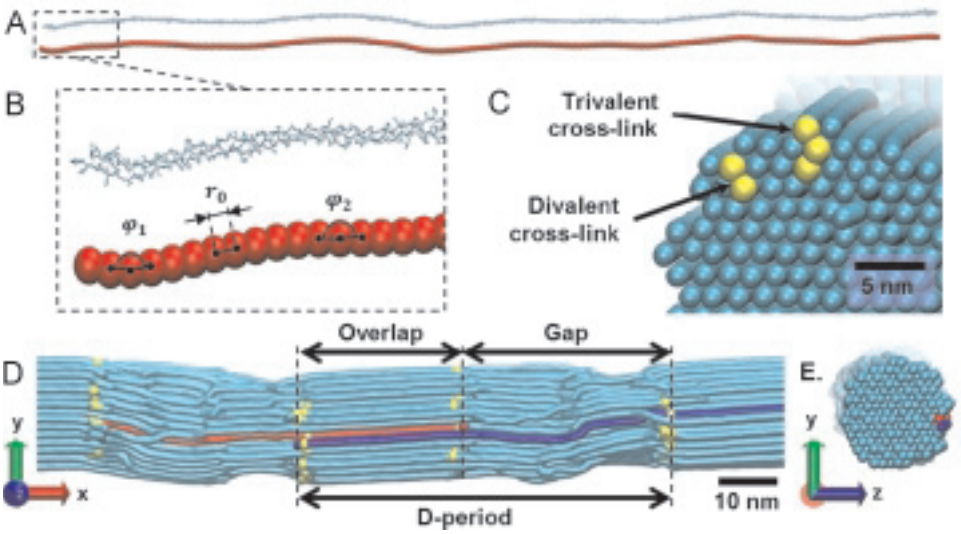

Fig. 1 – Creation of the collagen fibril coarse grained model. (A) Atomistic model of a single tropocollagen molecule (top) and its representation in the coarse-grained model (bottom). The molecule is 300 nm in length. Details of both models are shown in (B). (C) Example of divalent and trivalent cross-links in the coarse-grained model. (D) Coarse-grained model of a collagen fibril and (E) its cross-section. The two tropocollagen molecules in blue and red in (D) and (E) have been highlighted to show the staggering and entanglement of the molecules. The yellow beads represent the cross-linked particles as in (C).

the molecular geometry suggest that intermolecular enzymatic cross-links primarily develop between lysine or hydroxylysine residues at the ends of tropocollagen molecules (Viguet-Carrin et al., 2006; Eyre and Wu, 2005; Bailey et al., 1998; Robins and Bailey, 1977). Enzymatic cross-links form a covalent bond between side chains of the residues of two tropocollagen molecules. We study the influence of divalent and trivalent cross-links. Divalent and trivalent cross-links have been assumed to link two and three different collagen molecules respectively. Based on a distance criterion, the last bead of a collagen molecule forms a covalent bond with one or two adjacent molecules to create a divalent or a trivalent cross-link respectively. Fig. 1C shows a representation of the collagen cross-links in the model. The amount of both divalent and trivalent cross-links varies from 0 to 100% where 100% represents two terminal cross-links per collagen molecules (2 mol/mol), which is the maximum number of enzymatic cross-links that can be formed per molecule (Eyre and Wu, 2005). The distribution of the cross-links in the fibril is generated randomly.

2.3. Coarse-grained model parameterization of collagen molecules

The total energy of the system is given by the sum of all bond energy, three-body and pairwise interaction energy as

$$E_{\text{total}} = E_{\text{bond}} + E_{\text{angle}} + E_{\text{inter}} \tag{1}$$

where E_{bond} represent the energy contribution due to stretching, E_{angle}, the energy due to bending and E_{inter}, the energy due to intermolecular interactions. Each term is given by the sum of all the inter-bead interactions of this kind as

$$\begin{aligned} E_{\text{bond}} &= \sum_{\text{bonds}} \Phi_{\text{bond}}(r) \\ E_{\text{angle}} &= \sum_{\text{angles}} \Phi_{\text{angle}}(\varphi) \\ E_{\text{inter}} &= \sum_{\text{pairs}} \Phi_{\text{inter}}(r) \end{aligned} \tag{2}$$

The bonding energy contributions have been modeled with a bilinear law, to approximate the nonlinear stress-strain behavior of a single collagen molecule under tensile loading, as described previously (Buehler and Gao, 2006; Buehler and Wong, 2007). The force between two particles is

$$F_{\text{bond}}(r) = -\frac{\partial \Phi_{\text{bond}}(r)}{\partial r} \tag{3}$$

where:

$$\frac{\partial \Phi_{\text{bond}}(r)}{\partial r} = \begin{cases} k_T^{(0)}(r - r_0) & \text{if} \quad r < r_1 \\ k_T^{(1)}(r - r_0) & \text{if} \quad r_1 \le r < r_{\text{break}} \\ 0 & \text{if} \quad r > r_{\text{break}} \end{cases} \tag{4}$$

where $k_T^{(0)}$ and $k_T^{(1)}$ are spring constants for the small and large deformations. The stretching energy $\Phi_{\text{bond}}(r)$ is given by integrating $F_{\text{bond}}(r)$ over the radial distance.

The bending energy contributions of triplets of particles are defined by:

$$\Phi_{angle}(\varphi) = \tfrac{1}{2} k_B (\varphi - \varphi_i)^2 \tag{5}$$

where k_B has been computed based on the bending stiffness of the molecule (Buehler, 2006a, 2006b). The parameter φ_i represents the equilibrium angle between two beads of the coarse-grained model. Several different equilibrium angles have been selected in order to mimic a collagen molecule's initial geometry (Fig. 1B). The angles have been measured on the coarse-grained model representing a single collagen molecule and rounded to the nearest integer to reduce the number of variables. This results in eight equilibrium angles, ranging from 170 to 180°.

Intermolecular interactions are modeled by the Lennard–Jones (LJ) potential:

$$\Phi_{\text{inter}}(r) = 4\varepsilon_{LJ}\left[\left(\frac{\sigma_{LJ}}{r}\right)^{12} - \left(\frac{\sigma_{LJ}}{r}\right)^{6}\right] \tag{6}$$

where σ_{LJ} is the distance parameter and ε_{LJ} the energy parameter which determine the strength of the intermolecular adhesion without the presence of any cross-links (Buehler, 2006b).

The influence of water has been taken into account during the fitting of the coarse-grained parameters with full-atomistic results and is not explicitly modeled here. No viscosity has been included here and its influence will be analyzed in a subsequent study.

All coarse-grained parameters for solvated tropocollagen molecules are summarized in Table 1.

2.4. Coarse-grained model parameterization of cross-links

The cross-link properties are modeled using a bottom-up approach, in which we incorporate results from earlier work into the model. We selected two representative structures of divalent and trivalent cross-links (dehydro-lysino-norleucine and Lysyl-pyridinoline (Eyre and Wu, 2005)) and created a full atomistic model using Material studio 4.4 (Accelerys, Inc.) (Fig. 2). The mechanical behavior of the cross-links has been assessed by steered molecular dynamics in LAMMPS (Plimpton, 1995). Using ReaxFF reactive force field, we are able to evaluate the mechanical behavior of the cross-links until failure (Fig. 2).

For the trivalent cross-link, a tensile test has been performed in the three possible directions. Due to very similar behavior, the mechanical response of the cross-link has been averaged and fit to a single set of bond parameters in its coarse-grained representation. The responses of the cross-links have been assumed to be bilinear. Fibrils models have been built with the parameters of the cross-links presented in Table 1. To explore the influence of cross-links mechanical properties, we also build three fibril models with cross-links densities of 20%, 60% and 100% where the stiffness of the cross-links has been increased by multiplying the tensile stiffness parameters of trivalent cross-links by a factor two; all other parameters remain the same.

2.5. Simulation parameters and procedure

All molecular dynamics simulations are performed using the LAMMPS code (Plimpton, 1995). The integration time step is $\Delta t = 10$ fs. Equilibration calculation is carried out in NPT ensemble by applying Nose–Hoover thermostat set to 300 K and Hoover barostat set to 0 Pa along fibril length. Relaxation times for the thermostat and barostat are fixed to 1 and 10 ps respectively. Tensile loading is applied within the NVT ensemble. A single fibril is equilibrated in vacuum for 20 ns and the structure reaches the equilibrium state with no further

Table 1 – Summary of the parameters used in the mesoscopic molecular model of collagen (1 kcal mol^{-1} Å^{-1} = 69.479 pN).

System	Parameters	Value
Collagen	Equilibrium bead distance (r_0 Å)	14.00
	Critical hyperelastic distance (r_1, Å)	18.20
	Bond breaking distance (r_{break}, Å)	21.00
	Tensile stiffness parameter (k_0, kcal mol^{-1} Å^{-2})	17.13
	Tensile stiffness parameter (k_1, kcal mol^{-1} Å^{-2})	97.66
	Equilibrium angle, (θ_0, degree)	170.0 to 180.0
	Bending stiffness parameter (k_b, kcal mol^{-1} rad^{-2})	14.98
	Dispersive parameter (ϵ, kcal mol^{-1})	6.87
	Dispersive parameter (σ, Å)	14.72
Divalent cross-links	Equilibrium bead distance (r_0^d, Å)	10.00
	Critical hyperelastic distance (r_1^d, Å)	12.00
	Bond breaking distance (r_{break}^d, Å)	14.68
	Tensile stiffness parameter (k_0^d, kcal mol^{-1} Å^{-2})	0.20
	Tensile stiffness parameter (k_1^d, kcal mol^{-1} Å^{-2})	41.84
Trivalent cross-links	Equilibrium bead distance (r_0^t, Å)	8.60
	Critical hyperelastic distance (r_1^t, Å)	12.20
	Bond breaking distance (r_{break}^t, Å)	14.89
	Tensile stiffness parameter (k_0^t, kcal mol^{-1} Å^{-2})	0.20
	Tensile stiffness parameter (k_1^t, kcal mol^{-1} Å^{-2})	54.60
	Mass of each mesoscale particle, atomic mass units	1358.7

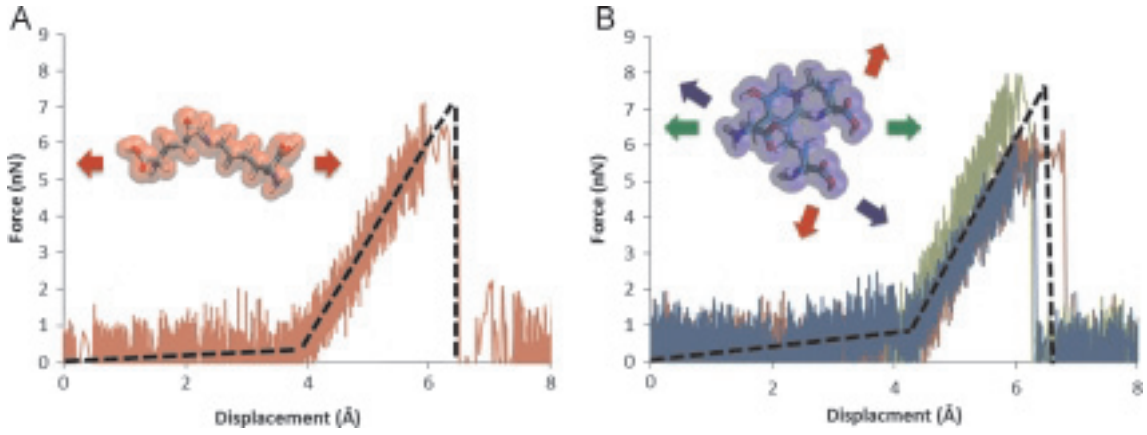

Fig. 2 – Characterization of cross-links mechanical properties. Force–displacement response of (A) divalent and (B) trivalent cross-links computed by full atomistic reactive molecular dynamics. The arrows on the atomistic representations of the cross-links represent the directions of the tensile tests performed on the molecules. The dashed lines correspond to the parameterization used in the mesoscale model.

structural change measured by root-mean-square deviation of bead positions. We also ensure that the fibril length after equilibration remains similar for all models to confirm the stability of the model and to prevent any folding of the fibril. Despite the relaxation along the fibril axis, the length variation between the different models is minimal (<0.35%). A visual test was performed in addition to guarantee the conservation of the fibrillar geometry. After equilibration calculation, the structure displays the characteristic D-period of collagen fibrils in agreement with experiments (Wenger et al., 2007; Hulmes et al., 1981; Hulmes, 2002). To model tensile deformation of collagen fibril we apply homogenous strain to the entire fibril model along the x-axis with the equivalent strain rate of 10^7 s^{-1} (3.3 m/s). This strain rate is five orders of magnitude larger than what is commonly used experimentally for stretching collagen material as the consequence of the timescale limitation of the molecular model. Total times spans of several microseconds are the most that can be simulated because of the small integration time step. We use the virial stress to compute the stress tensor (Tsai, 1979) for analysis of the strain–stress behavior of the fibril and collagen molecules.

2.6. *Visualization and data analysis*

The fibril models are created with Matlab R2010a (Mathworks Inc., Natick, MA).Visualization of the simulation is performed with VMD (Humphrey et al., 1996). Stress–strain curves are computed from the box size and the virial-stress of the particles given by the LAMMPS code.

3. Results

3.1. *Deformation and mechanical response of cross-linked collagen fibril in stretching*

To understand how collagen fibrils respond to stretching forces, we apply uniaxial tensile strain to deform the fibril model and record the reaction stress as a function of the applied strain. Stress-strain responses have been divided into up to five regions to facilitate the analysis of the mechanical response of the fibril (Fig. 3A). We obtain the toughness of the fibril by measuring the area under the stress-strain curve, until ultimate strength (as shown by the gray area in Fig. 3A). To compute the tangent modulus at various applied strains, we use a fifth order polynomial function to fit the stress-strain curve until ultimate strength as shown in Fig. 3A. We take the first derivative of the function to evaluate the modulus as shown in Fig. 3B. For a typical cross-linked fibril with normal cross-linked stiffness, the tangent modulus features two characteristic values. The modulus reaches a peak at small deformation (Mod1, 5–15% strain), followed by a minima (Mod2, 20–30% strain).

To better understand the nonlinear mechanics of the collagen fibril, we carefully investigate the mechanical response of tropocollagen molecules in stretching by analyzing the simulation trajectory. We correlate their molecular behavior with the overall force-extension curve, as shown by the simulation snapshots and schematic of their structural characteristic in Fig. 4. For strain lower than 2%, the samples display a characteristic toe region (Figs. 3A and 4, regime 0) corresponding to the straightening of the fibril, as seen in experimental studies (Svensson et al., 2013, 2012). The toe region is followed by an elastic deformation (regime I) until the yield of the fibril. In regime I, molecular stretching is the main deformation mechanism in the fibril (Figs. 4, regime I and 7). Intermolecular adhesion forces act as cohesive forces that allow a uniform deformation of the fibril, very similar to the behavior of a single collagen molecule (Buehler and Wong, 2007). This deformation regime corresponds to the uncoiling of the tropocollagen molecules as demonstrated in full-atomistic simulations (Buehler, 2006b). It accounts for about 80% of the deformation; the remaining 20% of deformation can be attributed to surface effects and molecule–molecule sliding.

Yielding occurs at strains around 10–15%. Past the yield point, the fibril exhibits a second regime (Fig. 4, regime II) characterized by a lower modulus. The stretching energy applied to the fibril exceeds the intermolecular interactions, which are not large enough to support the deformation of the structure, and the molecules start to slide along each other. The presence of cross-links restrains the sliding of the molecules and enhances the mechanical properties of the fibril when compared to pure collagen fibrils. In regime II, molecular sliding is combined with collagen molecules uncoiling.

Around 30% of deformation, fibrils reach their maximum stress when the first cross-links break. The cross-links rupture induces a relaxation of collagen molecules, which translates into a decrease of the molecular strain (Fig. 4, regime IV. Figs. 7 and 8). Failure of the fibril happens through the progressive intermolecular sliding and rupture of the cross-links that remain connected.

Before failure, fibrils with high trivalent cross-links density exhibit a third deformation regime (Fig. 4, regime III). This regime matches the point where collagen molecules reaches their second deformation regime characterized by a higher stiffness (Buehler, 2006b). At this point, molecular backbone stretching becomes the dominant mechanism of collagen molecules. This leads to a significant increase in the mechanical response of the fibril.

3.2. *Influence of cross-links type on fibril mechanics*

The stress-strain behaviors of collagen fibril containing divalent and trivalent cross-links with a stiffness calibrated on full atomistic simulations are shown in Fig. 5A and B respectively. Except for extreme cross-links densities, fibrils containing either divalent or trivalent cross-links present a similar bilinear

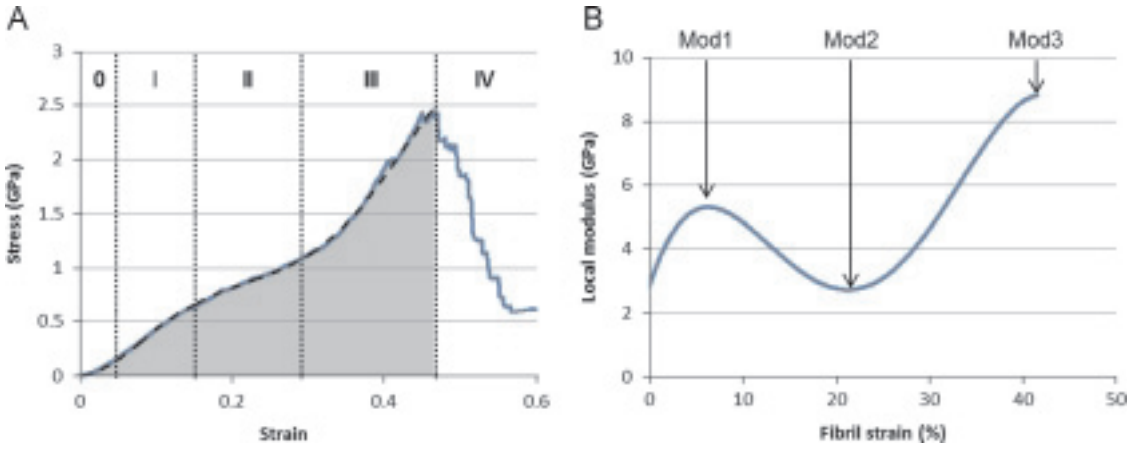

Fig. 3 – (A) Representative stress–strain response of a cross-linked collagen fibril. The dashed line represents the 5th order polynomial approximation used to compute the tangent modulus of the fibril along the deformation, as presented in panel B. Regions 0 to IV represent the different deformation mechanisms exhibited by the fibril. The gray area has been used to compute the fibril toughness. (B) Elastic modulus of the fibril as a function of the strain applied to the fibril. Region I, II and III reveal three distinct characteristic moduli, referred as Mod1, Mod2 and Mod3.

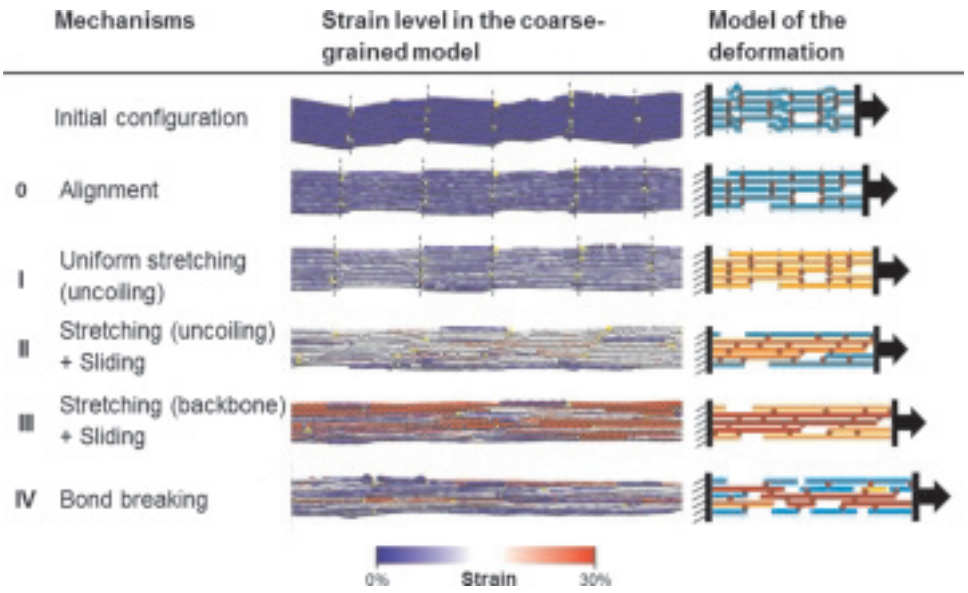

Fig. 4 – Representative deformation mechanisms and molecular strain level in a cross-linked collagen fibril (50% of cross-links). In the initial state, the fibril has a wavy shape, the cross-linked areas are contained in equidistant cross-sections of the fibril (dash lines). (0) The first 5% of the deformation correspond to the alignment of the fibril along the pulling direction, which leads to the toe region of the strain–stress curve. (I) The fibril enters an elastic regime where the collagen molecules display a higher strain level in the gap than in the overlap region because of the lower molecular density. (II) Around 15% of deformation, the sliding between the molecules becomes favorable. The molecules connected by the cross-links and forming the core of the fibril sustain most of the load. (III) If the strength of the cross-links is sufficient, the molecule stretching enters the deformation mode corresponding to the stretching of their backbone. (IV) The molecular stress exceeds the maximum stress bearable by either tropocollagen molecule or cross-links that start to break. Most of the molecules return to an unloaded state while conserving a residual stress.

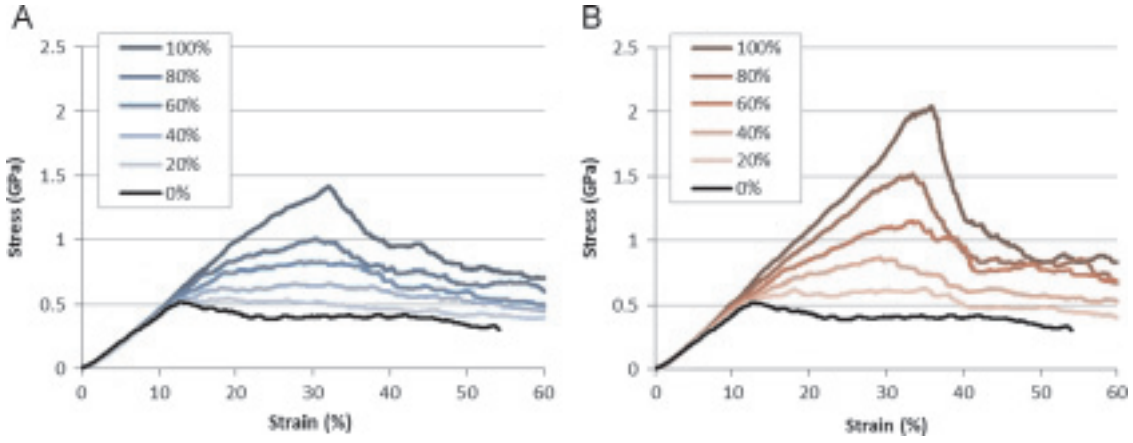

Fig. 5 – Stress–strain curve of a collagen fibril containing different density of (A) divalent and (B) trivalent cross-links. The results show that increasing the cross-link density leads to larger failure stress and toughness. For larger cross-links density, the second elastic regime of the tropocollagen molecules is activated. Fibrils with high trivalent cross-link density exhibit a more "brittle-like" behavior.

response before reaching their ultimate strength. For the same cross-link density, fibril stiffness, stress level and toughness are significantly increased in fibrils containing trivalent cross-links (Fig. 6A, B and D). For a given divalent cross-links density, these parameters are comparable to trivalent cross-link models with half the crosslink density. For example, the ultimate stress of a fibril containing 40% divalent cross-links is similar to that of a fibril containing 20% trivalent cross-links (0.63 versus 0.64 GPa). The difference of behavior between divalent and trivalent cross-links is due to a difference in connectivity of the molecular network; a fibril with certain amount of divalent cross-links will have similar connectivity as a fibril with half that amount of trivalent cross-links. The connectivity between collagen molecules created by the cross-links inside the fibril is therefore a major determinant of the fibril's mechanical properties.

3.3. *Influence of cross-links density on fibril mechanics*

The stress–strain curves for collagen fibril with various cross-link densities are shown Fig. 5. The first elastic regime presents an elastic modulus similar for all the samples of 5.19±0.34 GPa (Fig. 6A) confirming that cross-linking does not affect the tangential modulus of the fibrils (Li et al., 2013). Yielding occurs for a strain ranging from 5 to 10% depending on the cross-links density. In agreement with two dimensional coarse-grained models, yield strain and yield stress are dependent on cross-link density (Buehler, 2008). Cross-links delay intermolecular slippage and allow for further deformation of topocollagen molecules.

For a fibril containing low densities of cross-links (less than 60% divalent cross-links or less than 40% trivalent cross-links), the strain-stress response reaches a plateau around 0.5 GPa at the end of regime I and decreases progressively until total rupture, as reported in experiments (Svensson et al., 2013; Puxkandl et al., 2002). This plateau corresponds to the continuous molecular slippage occurring in the fibril since cross-link density is not large enough to prevent it. For larger densities, the fibril exhibits the two-phase behavior as presented in 3.1. In regime II, the deformation is a combination of intermolecular sliding and molecular uncoiling. The stiffness of this regime is directly proportional to the cross-link density (Fig. 6A). Indeed, by connecting the fibrils, the cross-links form a network of collagen molecules that can deform synergistically. This bundle of interconnected molecules forms the "core" of the fibril that will sustain most of post-yield deformation of the fibril. For a fibril reaching regime II with low cross-link densities, the fibril core is too small and poorly connected, and intermolecular sliding is the main deformation mechanism, which leads to a low stiffness of the structure. For higher concentrations of cross-links, the sliding becomes limited due to an increased connectivity in the structure and the fibril core sustains the deformation. The higher the cross-link density, the larger the fibril core will be leading to a higher stiffness of the structure.

In a fully cross-linked fibril (100% or 2 cross-link per molecules), most of the fibrils are inter-connected. As in regime I, all molecules stretch synergistically and no clear transition can be observed (Figs. 4A, 5B and 7B). A similar behavior has been observed experimentally where cross-links accumulation leads to a drastic reduction of fiber-sliding which is compensated by an increase in fiber-stretching (Li et al., 2013).

Most of the fibrils reaches their ultimate strength around 35% deformation, when the cross-links start to fail. The number of broken cross-links is proportional to the cross-link density (Fig. 8). Both the maximum stress and toughness of the fibril are linearly dependent on the cross-links density (Fig. 5B and D). Adding cross-links can significantly improve

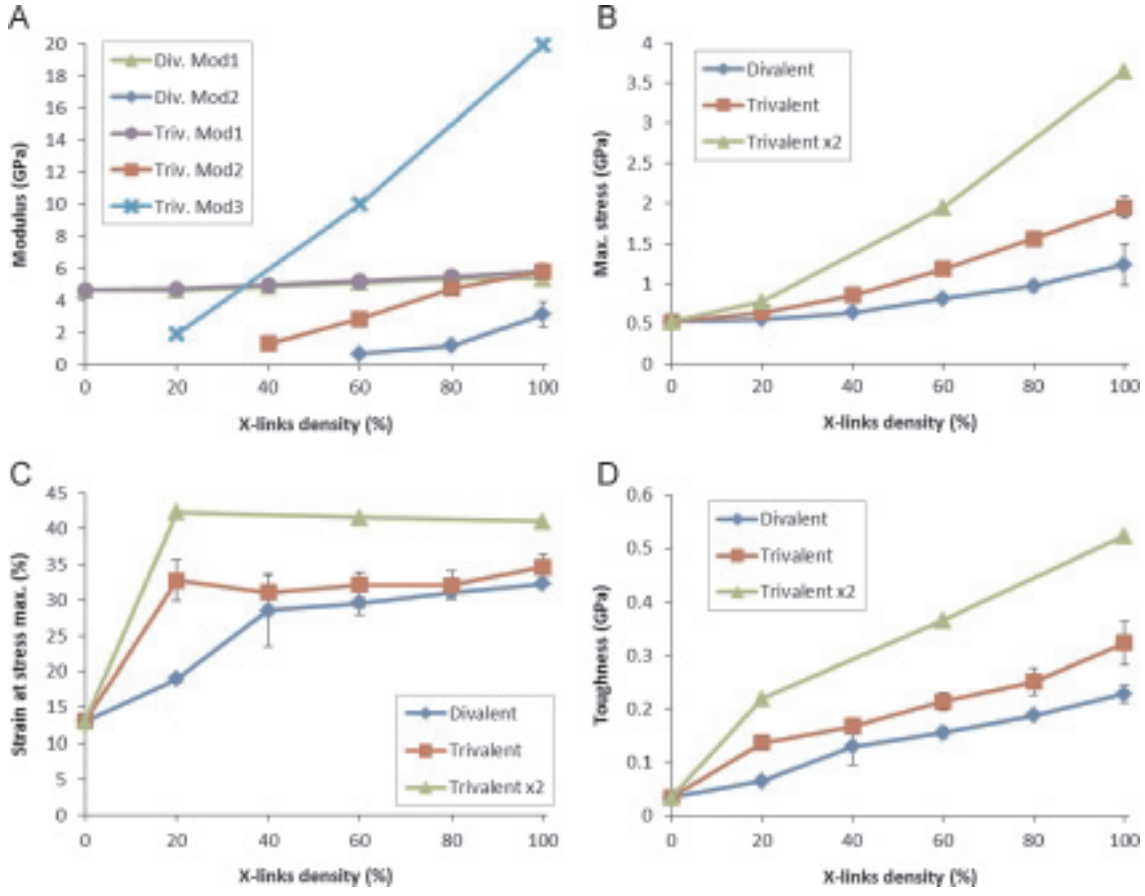

Fig. 6 – Change of the mechanical properties of a collagen fibril depending on the cross-link density and type. Trivalent cross-links with increased stiffness are noted trivalent × 2. (A) Characteristic moduli Mod1, Mod2 and Mod3, (B) maximum stress σ_F, (C) strain at maximum stress ε_F and (D) toughness of the fibril.

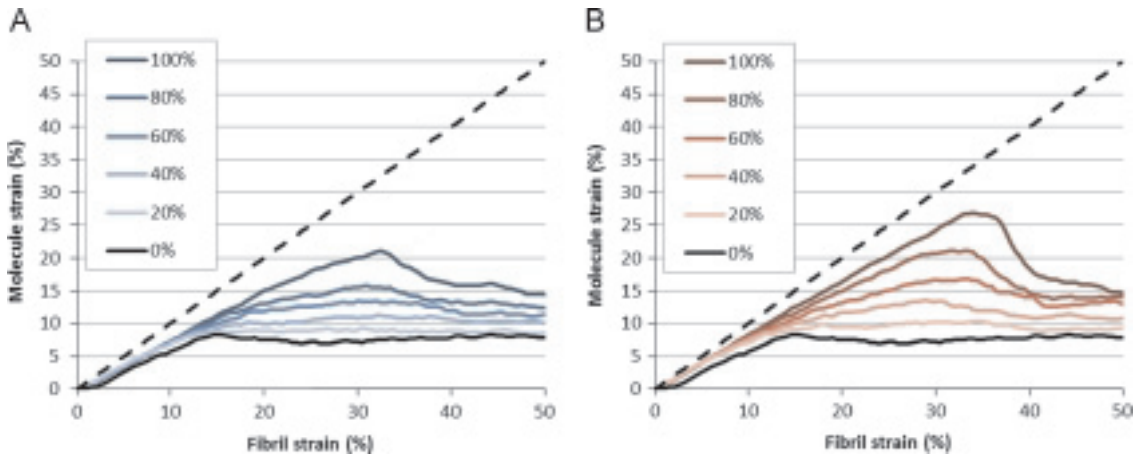

Fig. 7 – Average strain at the molecular level in fibrils containing various densities of divalent (A) and trivalent (B) cross-links. Below 10% strain, all tropocollagen molecules exhibit a similar deformation, which match pure collagen behavior. Beyond 10%, the cross-link's connective role is activated. For low cross-link density, molecule strain reaches a plateau as sliding becomes the predominant deformation mechanism. For higher densities, molecular strain keeps increasing linearly, proportional to the cross-link density. Between 40% and 50% deformation, molecular strain decreases as molecules start to break.

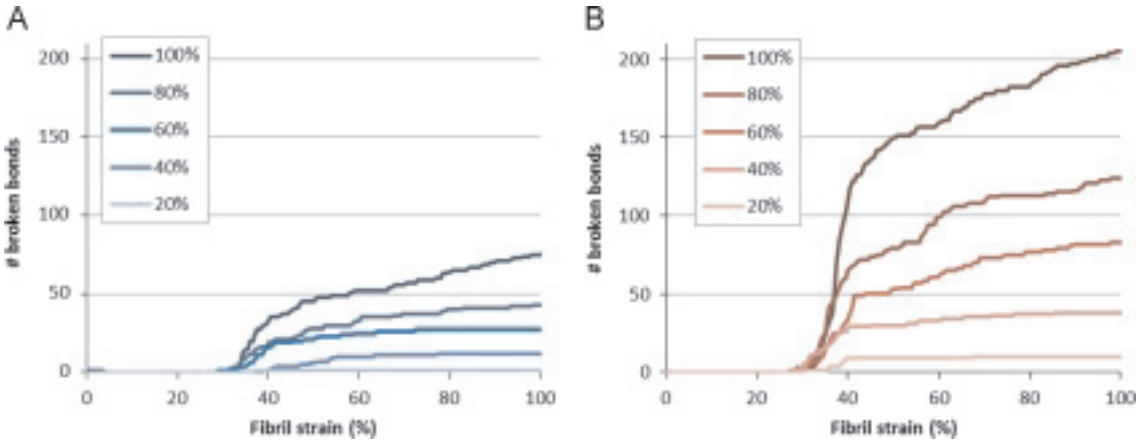

Fig. 8 – Evolution of the number of collagen broken bonds in the fibril as a function of applied strain, for varying density of (A) divalent and (B) trivalent cross-links. Collagen molecules start to break around 50% which corresponds to a single collagen molecule's maximum strain. The amount of broken molecules is proportional to the cross-link density.

the mechanical behavior of the fibril. The maximum stress can be increased up to 2.4 times for divalent cross-links and up to 3.8 times for trivalent cross-links (Fig. 6B). The toughness is also considerably increased and is up to 6.7 times the toughness of non-cross-linked collagen when considering divalent cross-links and up to 9.5 times for trivalent cross-links (Fig. 6D). Except for fibrils that do not exhibit regime II (low cross-links density), the collagen fibril reaches a constant fracture strain around 30% ($\varepsilon_F = 31 \pm 2\%$, Fig. 6C) showing that failure strain is not dependent on cross-link density.

3.4. *Influence of cross-links mechanical properties on fibril mechanics*

To study the role of cross-links mechanical properties on the fibril behavior, we double the cross-links tensile stiffness in the models containing 20%, 60% and 100% cross-links. The stress-strain responses of these models are presented in Fig. 9.

No significant difference can be observed in the response of the fibril until the end of the second regime showing that cross-links mechanics does not influence deformation regime I and II. The role of cross-links mechanics appears after 30% deformation where models with 60% and 100% cross-links exhibit a third deformation regime (Fig. 4, regime III, Mod3), similar to what have been observed in some experiments (Svensson et al., 2013). At this point, the collagen molecules forming the core of the fibril reach their second deformation regime. Molecular backbone stretching becomes the dominant mechanism of collagen molecules. Since backbone stretching is characterized by a larger stiffness, this leads to a stiffening of the structure. Similar to regime II, the stiffness of the third regime is dependent on fibril core size and therefore on cross-links density (Fig. 6A).

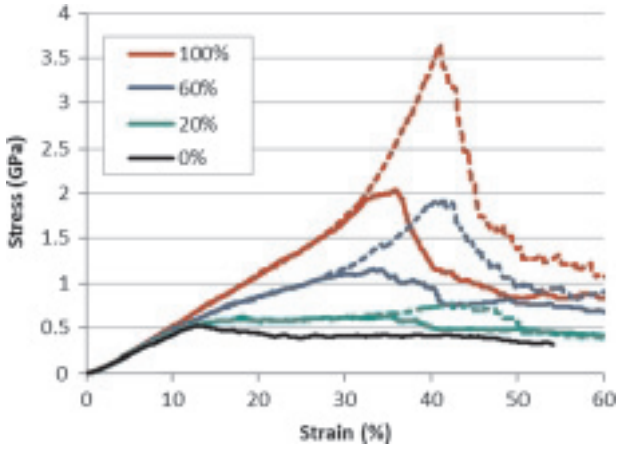

Fig. 9 – Stress–strain response of a collagen fibril containing different density of trivalent cross-links with normal (plain line) and increased cross-links strength (dashed line). Increasing cross-links strength leads to an increase of the failure strain of the fibril, which allow the fibril to enter its third deformation regime.

Increasing cross-links mechanics also impact the failure strain which increase to 42±1% (Fig. 6B) which approach the ultimate strain of a single collagen molecule (Buehler and Wong, 2007). A combination of collagen molecules and cross-links rupture leads to the failure of the fibril.

4. Discussion

This study explore the role of cross-links on the mechanics of type I collagen fibrils. Using a bottom up approach, we built a mesoscale model of cross-linked collagen fibril based on both accurate geometry and mechanical properties, allowing us to analyze the influence of cross-links type, density and mechanics on the fibril mechanical response. Under tension, cross-linked fibrils present up to three different deformation regimes. The cross-links density influences the stiffness of both the second and third deformation regimes. More cross-links induce a more well-connected structure that can deform synergistically and take advantage of the mechanical properties of each single tropocollagen molecules. On the other hand, cross-link mechanical properties determine the failure strain of the fibril. It also indirectly determines the presence of the third deformation regime at the fibril scale. Indeed, stronger cross-links allow collagen molecules to deform further, going beyond the complete uncoiling of the triple helix and reaching the stretching of the molecule backbone.

The deformation mechanisms of the collagen fibril described in this study are in good agreement with experimental data at the fibril level (Svensson et al., 2013, 2012). However, experimental results indicate that fibrils containing a majority of trivalent cross-links undergo a clear three phase mechanical response. With our model, the third deformation regime corresponding to the stiffening of the fibril is only observed for cross-links with increased strength. Assuming that the biological sample used experimentally did not withstand major structural changes during testing and that the measured cross-linked density is accurate, this could indicate that our model either underestimates cross-links mechanical properties or overestimate tropocollagen stiffness.

The good qualitative agreement of model with experiments shows that cross-linking alone is a major source of mechanical strength in connective tissue. The molecular model developed here allows us to explore the mechanisms behind the three-phase behavior observed experimentally during a tensile test of collagen fibril. The deformation mechanisms revealed in this study are in good agreement with previous full atomistic study of cross-links in the C-terminal domain of type I collagen (Uzel and Buehler, 2011), which also confirms the nonlinear three-phase behavior reported here, suggesting that the collagen molecules are assembled along their axis in a synergistic way.

From a quantitative point of view, our results slightly overestimate the mechanical properties of the fibril. Svensson et al. reported fibril moduli between 2.2 and 3.5 GPa for small-strain deformation (Mod1) and around 1.6 and 4.5 GPa for large-strain deformation (Mod2) of fibril containing divalent and trivalent cross-links respectively (Svensson et al., 2013). Eppell et al. reported values lower for the small-strain modulus (0.4–0.5 GPa) but higher for large-strain modulus (around 12 GPa) (Eppell et al., 2006). Our values are slightly larger for both small and large-strain modulus. Possible explanation for this disagreement could be entropic effects that may make the fibril softer, particularly in the small-deformation regime. Such entropic effects are partly taken into account in our model but could be significantly larger in experiments. The large deformation rates used in this study could also explain the differences. Indeed, atomistic modeling requires the usage of large deformation rate that often leads to overestimation of forces during mechanical deformation. Since the model used here is based on atomistic data, overestimation of the parameters obtained from molecular dynamic simulation would be transferred throughout to the multi-scale modeling scheme. Furthermore, the model described here represents fibrils with a diameter of 20 nm which is at least four to five times smaller compared to natural fibril used in experiments (between 80 and 100 nm in (Svensson et al., 2013)). A preliminary study revealed that for a diameter larger than 12 nm, the ultimate strength and tensile modulus of the fibrils are independent of its diameter (data not shown). Therefore, we believe that the fibril model used here is large enough to capture the deformation mechanisms of the structure. However, the size of the fibril could partly explain the high modulus compared to experimental values since size-dependent effects have been highlighted for collagen fibrils (Shen et al., 2008). Finally, our model represents perfect fibrils and does not take into account any variability of defect naturally occurring in biological samples. This is likely to lead to an over-estimation of the mechanics of the fibril. For that reason, our results should be taken as an upper boundary of the behavior of the collagen fibrils.

Another limitation here is that we only considered one type of cross-link per model. In nature, the cross-link distribution is more complex and combines divalent and trivalent cross-links of varying composition at the same time(Viguet-Carrin et al., 2006; Eyre and Wu, 2005). Cross-links issued from AGE are also

likely to influence the mechanical properties of the fibril and require further investigation. Here, we focus on the valence and amount of cross-linking and assume that the atomic structure does not largely influence the mechanical properties of the fibril. This is in contradiction with some experimental results that found some influence of the cross-link atomic composition on the global mechanical properties of bone tissue (Banse et al., 2002). However, in these experimental studies, it is possible that the measuring method employed does not make an inventory of all existing cross-links, making the relationship between cross-link concentration and mechanical properties indiscernible. Besides, the cross-link composition might induce some indirect modifications in the fibrillar structure that can be responsible for the alteration the mechanics of the fibril (modification in collagen molecules staggering, changes of the local molecular conformation or defaults in mineralization for bone tissue). The purpose of the variation in cross-link composition remains unclear. Some hypothesize that the valence of the cross-link is the most important factor in the strength of the fibril, the structure been more related to other behavior such as mineralization, turnover or thermal and chemical stability (Fratzl, 2008; Eyre and Wu, 2005; Bailey et al., 1998). Non-collagenous proteins (NCPs) might also play a role in the fibril mechanics. However, since most of the NCPs are found in the interfibrillar matrix (Cribb and Scott, 1995; Orgel et al., 2009; Nanci, 1999), we believe they do not play a major role in a single fibril mechanics.

This study supports the results of previous two-dimensional mesoscale models that found that cross-links govern large deformation and fracture mechanics of fibrils while its influence on small-deformation mechanics remains negligible (Buehler, 2008). Here we show that cross-links density and properties have two distinct roles on the fibril response, specifically the stiffness of large deformation regime for the former and failure strain for the latter. It also supports the idea that cross-links are essential to reach the second regime of collagen molecule deformation, corresponding to backbone stretching of the molecules. The present study also shows the importance of the three-dimensional organization of collagen molecules and cross-links in fibril mechanics, which had not been incorporated in the previous model.

Improved computational power allowed us to develop a model with finite size which can capture the deformation mechanisms taking place during the tensile deformation of the fibril. Indeed the 2D periodic sample could not carry size effect that is partly responsible for the third regime of the fibril. In earlier work, we also modeled the density variation by altering the adhesion forces at the end of each tropocollagen molecule. When compared to the present model, it can be related to a cross-link density of 100% (2 cross-links per molecules) with different cross-link strength. The discrete representation of the cross-links used in this study allows us to shed light on the formation of a core, which, as the backbone of the fibril, sustains most of the deformation. Such refinements allow us to mimic experimental results and to shed light on fibrillar deformation mechanisms.

Our results also support studies showing the influence of cross-linking in the mechanical behavior of bone tissue. Garnero et al. showed that an increase in the mature cross-link content was positively associated with an increase of ultimate stress and post-yield energy absorption (Garnero et al., 2006; Garnero, 2012). Similarly, a 50% decrease in trivalent cross-links is associated with a 26% and 30% reduction of the bending strength and modulus of cortical bone (Oxlund et al., 1995). In our model, a similar decrease (from 80% to 40% trivalent cross-links) leads to a reduction of 45% and 73% of the tensile strength and modulus of the fibril, respectively.

This study also proves that the maturation of enzymatic cross-links enhances the mechanical capabilities of the fibrils as discussed previously (Bailey et al., 1998). Compared to immature cross-links, the mature form leads to a twofold increase in the strength and a threefold increase in the toughness of the fibril for a comparable yield strain. On the other hand, the fibril reinforced with trivalent cross-links display a more brittle like behavior. The valence of the cross-link could be used to modulate the mechanical properties of the tissue. For example, fetal skin is composed predominantly of immature cross-links due to high turnover when greater flexibility is needed. During growth, the tissue is stabilized with more trivalent cross-links with a corresponding increase in its mechanical properties (Fratzl, 2008; Yamauchi et al., 1988).

5. Conclusion

In this study, we develop a three-dimensional coarse-grained model of cross-linked collagen fibrils, expanding on earlier work based on a two-dimensional model, and opening opportunities to explore many other properties such as bending or torsion, and finite size effects. By individually modeling each cross-link, we are able to explore the influence of cross-link properties on the mechanics of collagen fibrils. A cross-linked fibril undergoes a three phase behavior, allowing large deformation and energy dissipation: (i) an initial elastic deformation corresponding to the collagen molecule uncoiling, (ii) a linear regime where intermolecular sliding become predominant, and (iii) the second stiffer elastic regime which can be associated with the stretching of tropocollagen molecules backbone until the fibril ruptures. We report that the second and third regime stiffnesses are determined by intermolecular connectivity that is directly dependent on cross-links type (specifically their divalent or trivalent nature), and density. We also show a clear association between cross-links mechanical properties (stiffness and strength) and the presence of the third deformation regime and failure strain of the fibril. The results confirm earlier work that cross-link density governs post yield and large scale mechanics, and that cross-links strength governs failure strain. Altogether, density, type and mechanical properties of the cross-links have a large impact on the mechanical response of the fibril.

Acknowledgments

The authors gratefully acknowledge support from ONR, ARO and NSF. This work was supported by the Wellcome Trust grant WT097347MA.

REFERENCES

Andreassen, T., Seyer-Hansen, K., Bailey, A., 1981. Thermal stability, mechanical properties and reducible cross-links of rat tail tendon in experimental diabetes. Biochim. Biophys. Acta – Gen. Subj. 677, 313–317.

Bailey, A.J., Paul, R.G., Knott, L., 1998. Mechanisms of maturation and ageing of collagen. Mech. Ageing Dev. 106, 1–56.

Bailey, A.J., 2001. Molecular mechanisms of ageing in connective tissues. Mech. Ageing Dev. 122, 735–755.

Bourne, J.W., Torzilli, P.A., 2011. Molecular simulations predict novel collagen conformations during cross-link loading. Matrix Biol. 30, 356–360.

Buehler, M.J., 2007. Molecular nanomechanics of nascent bone: fibrillar toughening by mineralization. Nanotechnology 18, 295102.

Buehler, M.J., 2008. Nanomechanics of collagen fibrils under varying cross-link densities: atomistic and continuum studies. J. Mech. Behav. Biomed. Mater. 1, 59–67.

Buehler, M.J., 2006a. Nature designs tough collagen: explaining the nanostructure of collagen fibrils. Proc. Natl. Acad. Sci. USA 103, 12285–12290.

Buehler, M.J., 2006b. Atomistic and continuum modeling of mechanical properties of collagen: elasticity, fracture, and self-assembly. J. Mater. Res. 21, 1947–1961.

Buehler, M.J., Gao, H., 2006. Dynamical fracture instabilities due to local hyperelasticity at crack tips. Nature 439, 307–310.

Buehler, M.J., Wong, S.Y., 2007. Entropic elasticity controls nanomechanics of single tropocollagen molecules. Biophys. J. 93, 37–43.

Banse, X., Sims, T.J., Bailey, A.J., 2002. Mechanical properties of adult vertebral cancellous bone: correlation with collagen intermolecular cross-links. J. Bone Miner. Res. 17, 1621–1628.

Couppé, C., Hansen, P., Kongsgaard, M., Kovanen, V., Suetta, C., Aagaard, P., et al., 2009. Mechanical properties and collagen cross-linking of the patellar tendon in old and young men. J. Appl. Physiol. 107, 880–886.

Cribb, A.M., Scott, J.E., 1995. Tendon response to tensile stress: an ultrastructural investigation of collagen:proteoglycan interactions in stressed tendon. J. Anat. 187, 423–428.

Danielsen, C.C., Andreassen, T.T., 1988. Mechanical properties of rat tail tendon in relation to proximal-distal sampling position and age. J. Biomech. 21, 207–212.

Eyre, D., Wu, J., 2005. Collagen cross-links. Top. Curr. Chem. 247, 207–229.

Eppell, S.J., Smith, B.N., Kahn, H., Ballarini, R., 2006. Nano measurements with micro-devices: mechanical properties of hydrated collagen fibrils. J. R. Soc. Interface 3, 117–121.

Collagen: structure and mechanics. In: Fratzl, P (Ed.), Springer, New-York, NY.

Fessel, G., Snedeker, J.G., 2009. Evidence against proteoglycan mediated collagen fibril load transmission and dynamic viscoelasticity in tendon. Matrix Biol. 28, 503–510.

Gautieri, A., Vesentini, S., Redaelli, A., Buehler, M.J., 2011. Hierarchical structure and nanomechanics of collagen microfibrils from the atomistic scale up. Nano Lett. 11, 757–766.

Gautieri, A., Redaelli, A., Buehler, M.J., Vesentini, S., 2014. Age- and diabetes-related nonenzymatic crosslinks in collagen fibrils: candidate amino acids involved in Advanced Glycation End-products. Matrix Biol. 34, 89–95.

Galeski, A., Kastelic, J., Baer, E., Kohn, R.R., 1977. Mechanical and structural changes in rat tail tendon induced by alloxan diabetes and aging. J. Biomech. 10, 775–782.

Garnero, P., 2012. The contribution of collagen crosslinks to bone strength. Bonekey Rep. 1, 182.

Garnero, P., Borel, O., Gineyts, E., Duboeuf, F., Solberg, H., Bouxsein, M.L., et al., 2006. Extracellular post-translational modifications of collagen are major determinants of biomechanical properties of fetal bovine cortical bone. Bone 38, 300–309.

Hulmes, D., Jesior, J.C., Miller, A., Berthet-Colominas, C., Wolff, C., 1981. Electron microscopy shows periodic structure in collagen fibril cross sections. Proc. Natl. Acad. Sci. 78, 3567.

Hulmes, D.J.S., 2002. Building collagen molecules, fibrils, and suprafibrillar structures. J. Struct. Biol. 137, 2–10.

Humphrey, W., Dalke, A., Schulten, K., 1996. VMD: visual molecular dynamics. J. Mol. Graph 14 (33–8), 27–28.

Orgel, JPRO, Eid, A., Antipova, O., Bella, J., Scott, J.E., 2009. Decorin core protein (decoron) shape complements collagen fibril surface structure and mediates its binding. PLoS One 4, e7028.

Kadler, K.E., Baldock, C., Bella, J., Boot-Handford, R.P., 2007. Collagens at a glance. J. Cell Sci. 120, 1955–1958.

Knott, L., Bailey, A.J., 1998. Collagen cross-links in mineralizing tissues: a review of their chemistry, function, and clinical relevance. Bone 22, 181–187.

Li, Y., Fessel, G., Georgiadis, M., Snedeker, J.G., 2013. Advanced glycation end-products diminish tendon collagen fiber sliding. Matrix Biol. 32, 169–177.

Nair, A.K., Gautieri, A., Chang, S.-W., Buehler, M.J., 2013. Molecular mechanics of mineralized collagen fibrils in bone. Nat. Commun. 4, 1724.

Nanci, a., 1999. Content and distribution of noncollagenous matrix proteins in bone and cementum: relationship to speed of formation and collagen packing density. J. Struct. Biol. 126, 256–269.

Ottani, V., Martini, D., Franchi, M., Ruggeri, a., Raspanti, M., 2002. Hierarchical structures in fibrillar collagens. Micron 33, 587–596.

Orgel, JPRO, Irving, T.C., Miller, A., Wess, T.J., 2006. Microfibrillar structure of type I collagen in situ. Proc. Natl. Acad. Sci. USA 103, 9001–9005.

Oxlund, H., Barckman, M., Ørtoft, G., Andreassen, T., 1995. Reduced concentrations of collagen cross-links are associated with reduced strength of bone. Bone 17, 365–371.

Parry, D.A., Craig, A.S., 1977. Quantitative electron microscope observations of the collagen fibrils in rat-tail tendon. Biopolymers 16, 1015–1031.

Plimpton, S., 1995. Fast parallel algorithms for short-range molecular dynamics. J. Comput. Phys. 117, 1–19.

Puxkandl, R., Zizak, I., Paris, O., Keckes, J., Tesch, W., Bernstorff, S., et al., 2002. Viscoelastic properties of collagen: synchrotron radiation investigations and structural model. Philos. Trans. R. Soc. Lond. B Biol. Sci. 357, 191–197.

Rigozzi, S., Müller, R., Stemmer, A., Snedeker, J.G., 2013. Tendon glycosaminoglycan proteoglycan sidechains promote collagen fibril sliding-AFM observations at the nanoscale. J. Biomech. 46, 813–818.

Robins, S., Bailey, A., 1977. The chemistry of the collagen cross-links. Biochem. J. 163, 339–346.

Shoulders, M.D., Raines, R.T., 2009. Collagen structure and stability. Annu. Rev. Biochem. 78, 929.

Svensson, R.B., Mulder, H., Kovanen, V., Magnusson, S.P., 2013. Fracture mechanics of collagen fibrils: influence of natural cross-links. Biophys. J. 104, 2476–2484.

Saito, M., Marumo, K., Fujii, K., Ishioka, N., 1997. Single-column high-performance liquid chromatographic-fluorescence detection of immature, mature, and senescent cross-links of collagen. Anal. Biochem. 253, 26–32.

Svensson, R.B., Hansen, P., Hassenkam, T., Haraldsson, B.T., Aagaard, P., Kovanen, V., et al., 2012. Mechanical properties of human patellar tendon at the hierarchical levels of tendon and fibril. J. Appl. Physiol. 112, 419–426.

Siegmund, T., Allen, M.R., Burr, D.B., 2008. Failure of mineralized collagen fibrils: modeling the role of collagen cross-linking. J. Biomech. 41, 1427–1435.
Shen, Z.L., Dodge, M.R., Kahn, H., Ballarini, R., Eppell, S.J., 2008. Stress-strain experiments on individual collagen fibrils. Biophys. J. 95, 3956–3963.
Tanzer, M., 1968. Intermolecular cross-links in reconstituted collagen fibrils evidence for the nature of the covalent bonds. J. Biol. Chem. 243, 4045–4054.
Tang, S.Y., Vashishth, D., 2011. The relative contributions of non-enzymatic glycation and cortical porosity on the fracture toughness of aging bone. J. Biomech. 44, 330–336.
Tsai, D.H., 1979. The virial theorem and stress calculation in molecular dynamics. J. Chem. Phys. 70, 1375.
Uzel, S.G.M., Buehler, M.J., 2011. Molecular structure, mechanical behavior and failure mechanism of the C-terminal cross-link domain in type I collagen. J. Mech. Behav. Biomed. Mater. 4, 153–161.
Van der Rest, M., Garrone, R., 1991. Collagen family of proteins. FASEB J. 5, 2814–2823.
Viguet-Carrin, S., Garnero, P., Delmas, P., 2006. The role of collagen in bone strength. Osteoporos. Int. 17, 319–336.
Verzijl, N., DeGroot, J., Ben, Z.C., Brau-Benjamin, O., Maroudas, A., Bank, R.A., et al., 2002. Crosslinking by advanced glycation end products increases the stiffness of the collagen network in human articular cartilage: a possible mechanism through which age is a risk factor for osteoarthritis. Arthritis Rheum. 46, 114–123.
Viguet-Carrin, S., Follet, H., Gineyts, E., Roux, J.P., Munoz, F., Chapurlat, R., et al., 2010. Association between collagen cross-links and trabecular microarchitecture properties of human vertebral bone. Bone 46, 342–347.
Wang, X., Shen, X., Li, X., Mauli Agrawal, C., 2002. Age-related changes in the collagen network and toughness of bone. Bone 31, 1–7.
Wenger, M.P.E., Bozec, L., Horton, M.A., Mesquida, P., 2007. Mechanical properties of collagen fibrils. Biophys. J. 93, 1255–1263.
Yang, L., van der Werf, K.O., Dijkstra, P.J., Feijen, J., Bennink, M.L., 2012. Micromechanical analysis of native and cross-linked collagen type I fibrils supports the existence of microfibrils. J. Mech. Behav. Biomed. Mater. 6, 148–158.
Yamauchi, M, Woodley, D, Mechanic, G., 1988. Aging and cross-linking of skin collagen. Biochem. Biophys. Res. Commun. 152, 898–903.
Zimmermann, E a, Schaible, E, Bale, H, Barth, HD, Tang, SY, Reichert, P, et al., 2011. Age-related changes in the plasticity and toughness of human cortical bone at multiple length scales. Proc. Natl. Acad. Sci. USA 108, 14416–14421.